In vitro Response of Human Osteoblasts Cultured on Strontium Substituted Hydroxyapatites

SORIN RAPUNTEAN[1], PETRE T. FRANGOPOL[2], IOANA HODISAN[2,3], GHEORGHE TOMOAIA[4,5], DANIEL OLTEAN-DAN[4], AURORA MOCANU[2], CRISTINA PREJMEREAN[6], OLGA SORITAU[7], LEVENTE ZSOLT RACZ[2,*], MARIA TOMOAIA-COTISEL[2,5*]

[1]University of Agricultural Sciences and Veterinary Medicine of Cluj-Napoca, 3-5, Manastur Str., 400372, Cluj-Napoca, Romania
[2]Babes-Bolyai University of Cluj-Napoca, Faculty of Chemistry and Chemical Engineering, Physical Chemistry Centre, 11 Arany J. Str., 400028, Cluj-Napoca, Romania
[3]Iuliu Hatieganu University of Medicine and Pharmacy, Faculty of Dental Medicine of Cluj-Napoca, 8 Victor Babes Str., 400012, Cluj-Napoca, Romania
[4]Iuliu Hatieganu University of Medicine and Pharmacy, Orthopedy and Traumatology Department, 47 Mosoiu T. Str., 400132, Cluj-Napoca, Romania
[5]Academy of Romanian Scientists, 54 Splaiul Independentei, 050094, Bucharest, Romania
[6]BabesBolyai University, Raluca Ripan Institute of Research in Chemistry, 30 Fantanele Str., 400294, Cluj-Napoca, Romania
[7]Oncology Institute of Cluj-Napoca, 34-36 Republicii Str., 400015 Cluj-Napoca, Romania

The goal of this study was to analyze the response of osteoblasts cultured on strontium substituted hydroxyapatites (HAP-Sr) of well-defined high crystallinity deposited as thin films on glass plates. Up to now, this aspect has not been carefully investigated in the context of bio-ceramics. In this study, we present the osteoblasts activity on synthesized HAP-Sr for different amounts of strontium substitution for calcium within the hydroxyapatite ($Ca_{10}(PO_4)_6(OH)_2$, HAP) lattice, namely HAP-5%Sr, HAP-10%Sr, HAP-15%Sr and HAP-59.2%Sr (Sr-HAP, of formula $Sr_{10}(PO_4)_6(OH)_2$), in comparison with stoichiometric pure HAP, chosen as control. Each bio-ceramic was deposited as thin multilayers self-assembled substrate (scaffold) and chemically bonded to the surface of glass plates. These coatings revealed by AFM and SEM imaging a granular texture formed from bio-ceramic nanoparticles. They possessed a high degree of crystallinity, i.e. 68% to 86%, depending on the Sr amount within the HAP lattice, as judged by XRD. Osteoblasts were cultured up to 21days and displayed enhanced adhesion and proliferation particularly evidenced on relatively high strontium contents (especially 5 and 10 weight %, determined by SEM-EDX), where the alkaline phosphatase activity and type I collagen were strongly evidenced. These bio-ceramics showed a high in vitro biocompatibility stimulating the activity of osteoblasts in the process of bone formation. These nano biomaterials can have applications in orthopedic and dental surgery improving the osteointegration as coatings of bone implants as well as for bone repair and regeneration.

Keywords: ceramics, strontium substituted hydroxyapatite, osteoblasts, alkaline phosphatase activity, collagen, cellular viability

The healing of fractures requires the use of biocompatible materials with specific physical and chemical properties as well as osteoconductive and bone regeneration capacity [1- 16]. In orthopedic surgery, a more difficult situation is associated with bone fragility, like osteoporosis [17, 18], where a special attention is required concerning the selection of the graft material.

Despite of existence of many commercial bone grafts, such as stainless steel and titanium, they cannot regenerate healthy bone, due to the formation of a common fibrous tissue at the interface between graft and host tissue and the development of non-specific immune response. Therefore, surface active glasses enriched in strontium, Sr, [19-21] have received attention particularly to avoid the host immune response and to enhance the local mineralisation due to their ability to induce hydroxyapatite formation and crystallization.

Furthermore, the increasing interest in the development of bio-ceramics based on synthetic hydroxyapatite (HAP) and substituted HAP with various essential elements, such as Mg, Zn, Si and Sr [4-16] and especially for Sr substituted HAP (HAP-Sr) [11-13, 22-28], for bone repair is justified by the growing evidence of Sr beneficial effect on bone regeneration [2, 17, 20].

These bioactive materials are intensively investigated in terms of inducing fast osseointegration with host bone by promoting cell proliferation and differentiation as well by activating specific signalling pathways [18] and gene expression. Undoubtedly, the incorporation of physiological ions such as strontium, zinc, magnesium, silicate in bone grafts is of specific interest due to their role in bone metabolic processes [19, 21].

Moreover, the ions of Ca^{2+} and Sr^{2+} incorporated in bioactive ceramics, as in Sr partially substituted HAP, can activate the intracellular signalling pathways coordinated by calcium-sensing receptor in bone cells leading to an increased recruitment, proliferation, differentiation and survival of osteoblasts [18, 29].

In this work we aimed to investigate the *in vitro* biocompatibility and osteoconductive ability of different substrates made of synthetic HAP substituted with various amounts of Sr (e.g., 0, 5, 10, 15 and 59.2%), using human osteoblasts [30].

Experimental part

Materials and methods

Materials and chemical reagents for synthesis of hydroxyapatite and Sr substituted hydroxyapatite were of analytical grade and were purchased from various suppliers, such as from Sigma-Aldrich and Merck. The Dulbecco's modified Eagle's medium (DMEM), F12 Ham medium and various supplements for cell culture, fetal

* email: raczlevi90@gmail.com; mcotisel@gmail.com

bovine serum (FBS), L-glutamine, penicillin and streptomycin solution, non-essential aminoacids (NEA), dexamethasone, β-glycerol-phosphate, ascorbic acid were purchased from Sigma-Aldrich. All other reagents, including fluorescein diacetate, Hank's isotonic balanced salt solution, trypsin-EDTA, and phosphate buffered saline (PBS), were purchased from Sigma. Alamar blue and collagenase IV were purchased from Invitrogen, Thermo Fisher Scientific. Deionized ultrapure water was used in all experiments. All chemicals were used as received.

Synthesis of pure HAP and Sr substituted HAP

High purity stoichiometric nano hydroxyapatite, HAP: $Ca_{10}(PO_4)_6(OH)_2$, and strontium substituted nano hydroxyapatites, HAP-Sr, for different Sr amounts: HAP-5wt%Sr; HAP-10wt%Sr; HAP-15wt%Sr; HAP-59.2wt%Sr (i.e., Sr-HAP: $Sr_{10}(PO_4)_6(OH)_2$), were synthesized by wet chemical methodology, assisted by template compounds. After lyophilization, the organic templates were removed by calcination in two steps, at 550 °C for 6h and then at 850 °C for 4h. The obtained nano powders were thoroughly characterized as previously presented [11].

Preparation of HAP and HAP-Sr multilayered substrates

Self-assembled nanostructured substrates of HAP or HAP-Sr were prepared by the layer by layer method, as previously described [6, 8]. Briefly, a layer of a certain substrate was obtained by its adsorption from its aqueous dispersion on flat glass support, previously activated with hydrochloric acid solution. The resulted adsorbed layer of bio-ceramic was further washed with aqueous solution of sodium silicate, several times, to assure strong interactions between the adsorbed layers of chosen substrate material. Then, another adsorbed layer of bio-ceramic was built. Finally, at least 10 adsorbed layers were periodically self-assembled as a whole substrate (thin scaffold), which was thoroughly washed in pure water and dried at room temperature. These substrates showed good stability in cell culture, since a significant lost of scaffold material was not observed by dissolution in cellular medium during three weeks of experiments. The surface morphology of these substrates was examined by SEM and AFM [31-38]. Then, after the traditional sterilization in ethylene oxide [6, 8] these substrates were investigated in cell culture for at least 21 days (21d).

Characterization methods

Field emission *scanning electron microscope* (*SEM*), Hitachi SU-8230, operated at 30 kV, was used to explore the nanostructure of HAP and HAP-Sr substrates. SEM was equipped with Oxford energy-dispersive X-ray spectrometer (EDS) for elemental analysis (energy-dispersive X-ray, EDX spectra). SEM grids were of Cu, covered by a carbon layer of 10 to 20 nm thickness. SEM samples were prepared by deposition of HAP and HAP-Sr in thin layers on SEM grids. SEM-EDS equipment was used on substrates for elemental analysis.

Atomic force microscopy (AFM) images were obtained using an AFM JEOL 4210 equipment, operated in tapping mode, using standard cantilevers with silicon nitride tips (resonant frequency in the range of 200-300 kHz, spring constant 17.5 N/m). The particles were adsorbed from their aqueous dispersion on optically polished glass support, chemically activated with hydrochloric acid solution. The aqueous dispersions of HAP or HAP-Sr were homogenized using a high-intensity ultrasonic processor Sonics Vibra-Cell, model VCX 750, for 50 min, at room temperature around 22 °C.

Carl Zeiss AG Axio Observer D1 fluorescence inverted Microscope equipped with AxioCam MRC Digital Camera, and Axiovision Release 4.6.3. software C (Carl Zeiss Promenade 10, 07745 Jena, Germany, Carl Zeiss Microscopy GmbH).

BioTek Synergy 2 plate reader, with monochromator, wavelength range 200-999 nm, 3 fluorescence filters, Gen5 Data Analysis Software included (Kocherwaldstr. 34, D-74177 Bad Friedrichshall, Germany).

In vitro biocompatibility studies

Human Osteoblasts

Human osteoblast-like cells were isolated from bone explants (femoral heads after total hip replacement surgery) pieces in the Orthopedic Clinic, Cluj-Napoca. The donor received an informed consent for the use of the waste cells or tissues in the academic research. Bone fragments were harvested in DMEM/F-12Ham complete medium. The fragments were mechanically processed with forceps in small pieces (of approximately 3mm x 3mm) and washed extensively with PBS (phosphate buffer saline-Sigma) to remove blood cells and debris with a final wash in culture medium. We used a modified protocol described by Gallagher [30]. The bone fragments were exposed 30 min to an enzymatic digestive cocktail composed of 0.1% collagenase IV (Gibco) plus 0.25% trypsin EDTA (Sigma) and the enzymes' activity was stopped by subsequently washings by centrifugation with complete DMEM/ F-12 medium containing 10% FCS (fetal bovine serum-Sigma). Cell suspension was filtered using Filcons devices with 70 µm mesh. Bone explants and isolated cells were cultured in complete Dulbecco's modified Eagle's medium (DMEM) / F-12Ham (Sigma Aldrich) containing 20% FBS (fetal bovine serum), 2mM L-glutamine, 1% antibiotics, 1% non-essential aminoacids (NEA) (all reagents from Sigma), in 25-cm^2 culture flasks (Nunclon Thermo-scientific) in a humidified incubator with 7% CO_2 atmosphere, at 37°C. Medium was changed every 2 days. After 14 days the first spindle-like cells appeared and after 6–8 weeks, when the culture reached confluence, the bone fragments were discarded and cells were harvested using trypsin EDTA. Further, the adherent cells were detached by trypsinization and the first passage was initiated. Briefly, after 3 washes with PBS, cells' monolayer was exposed to trypsin EDTA solution for 5 min at 37°C, and afterwards the enzyme activity was inhibited with medium containing 10% FBS. Cell suspension was centrifuged for 5 min at 1100 rpm, and the cell pellet was re-suspended in complete DMEM medium and seeded into Cole flasks.

Then, the cultivation medium was the same as for the primary culture with 10% FBS. Isolated cells were characterized for markers of bone cells, osteopontin and osteonectin by immunocytochemical staining at the 3th passage. For in vitro biocompatibility and differentiation experiments, isolated osteoblasts were used after the sixth passage, when the cell cultures showed a stable cell morphology with a good proliferation degree.

Cells were seeded onto each sterilized ceramic substrate (scaffold) self-assembled on glass cover slides (18mm x 18mm) using as control, cells cultivated on pure HAP substrates. The ceramic substrates were placed in the 6 well plates. Cells were seeded in 3 mL/well complete DMEM medium at a density of $2x10^5$ cells/well. Medium was changed every 2 days.

Fluorescein diacetate cell adhesion and viability assay

Fluorescein diacetate, FDA, is used to detect cell adhesion and as a fluorescent indicator of cell viability. The FDA is

the substrate for the intracellular nonspecific esterase, and it freely diffuses into cells and is rapidly hydrolysed to fluorescein once it enters into a viable cell. The intensity of fluorescence is dependent on membrane integrity and enzymatic activity of the cells, so the fluorescent signals are proportional with the number and size of viable cells. The $2x10^5$ osteoblasts were seeded in each well of the 6-well plates, namely in 3 mL complete DMEM medium/ well on the surface of each specific coating substrate (scaffold). After 1.5, 24 h (1d), and 3d the cell viability (adhesion, proliferation and function of osteoblasts) was analysed using FDA assay. Briefly, osteoblasts were incubated 5 min in dark at 37°C with 1mL /well of FDA solution (at a final concentration of 2.4 mM in phosphate buffer saline, PBS) supplemented with Ca^{2+} and Mg^{2+}. After incubation the wells were washed twice with PBS, and viable fluorescent cells adhered on scaffolds were visualized with a Zeiss Axio Observer D1 inverted fluorescence microscope using a 488nm excitation filter. Images were captured with a CCD camera (Axiocam MRM) and analyzed using Axiovision Release 4.6.3. software.

Alamar Blue cell viability assay

After the seeding of cells on bio-ceramic substrates, cell adhesion in the first six hours (6h) and cells' proliferation can be assessed by Alamar Blue assay, which is used mainly as a test of cell viability. Alamar Blue is a cell viability reagent which contains the cell permeable, non-toxic and weakly fluorescent blue indicator dye, called resazurin. In metabolically active cells, resazurin is converted to resorufin, a red highly fluorescent dye, through a reduction mechanism. Fluorescence intensity depends on the number of viable cells. Thus, Alamar Blue assay is useful for quantitatively measuring the cell proliferation and mitochondrial metabolic activity. The $2x10^5$ osteoblasts were suspended in 1 mL of complete DMEM medium and seeded on the surface of each bio-ceramic substrate (scaffold) placed in 6-well plates. Each determination was performed in six independent experiments. After 6h of cultivation time, required for initiating the process of cell adhesion, 100ìl of Alamar Blue (Invitrogen) was added to each well (with a final concentration of 1/10). The plates are incubated for 1 hour at 37° C, in the dark. Then, medium aliquots were transferred to another 12-well plate and fluorescence intensity was measured using a BioTek Synergy 2 plate reader (excitation 540 nm, emission 620 nm). Cell viability and cell proliferation were evaluated in the same way after 24 h (1d), 3d, 5d and 12d of the cultivation of osteoblasts onto the surface of each bio-ceramic substrate.

The fluorescence intensity values depend on the number of viable cells and are related with each substrate used and with the established incubation time. The fluorescence intensity, corresponding to the initial cell number (2×10^5 cells/well) seeded on control pure HAP substrate, is taken as 100% at each time point investigated. Then, 6 wells were examined for each selected scaffold, and for each independent experiment. The fluorescence intensity obtained for each HAP-Sr substrate at a specific time point was evaluated accordingly to the % control.

Assessing the mineralisation process

Soluble type 1 collagen detection with Sircol test

The Sircol assay is a dye-binding method and measures acid-soluble and pepsin-soluble type 1 collagen that has not yet been cross linked. The Sircol assay can assess the newly synthesised collagen produced during rapid cellular growth and development periods *in-vitro* cell culture. This assay can also measure *in vitro* extracellular matrix formation. Therefore, the *dye Sirius Red binds* to collagen type I, giving the red-colored product in which the *bound dye* is proportional to the amount of fibrillary collagen. Each experiment was independently repeated for six times, following the full instructions from Sircol kit.

Cell culture media were collected at different points of time and stored at -80°C. The Sirius Red dye-binding method was used for measuring the acid-soluble and pepsin-soluble collagen, named Sircol test (Biocolor Ltd. Life Science Assays). The 100mL of test samples (or control samples) of culture media from cells cultivated on substrates were added to 1.5 mL micro-centrifuge tubes, in duplicates. Control samples consist from culture media without cells and without substrates. Each experiment was repeated for six times. For obtaining standard curve, the collagen standards were prepared, by solving reference standard (collagen 500mg/mL) in deionised water. The 1mL of Sircol dye reagent was added to each tube and then the samples were placed in a mechanical shaker for 30 min. Samples were centrifuged at 12 000 rpm for 10 min, and the supernatant was discarded and unbound dye was removed. To the collagen-dye pellets was added 750µL of ice-cold Acid Salt wash reagent to remove unbound dye, and samples were centrifuged at 12 000rpm for 10 min. After draining the microtubes, 250 µL of Alkali reagent (0.5M sodium hydroxide) was added to microtubes and the bound dye was dissolved by vortexing within 5min. The 200µL of each sample was transferred to individual well of a 96 well microplate, and absorbance was measured with BioTek Synergy 2 microplate reader at 555nm.

Data were normalized to the collagen amount, as measured using HAP control scaffold, expressed as µg/ mL, and was taken as 100%, at the first time point (5days) investigated. The collagen amount obtained for each ceramic substrate at a specific time point was evaluated accordingly to the % control.

Alkaline phosphatase activity

For measurement of alkaline phosphatase activity a fluorescent alkaline phosphatase detection kit (Sigma-Aldrich) was used. Cell culture medium collected at different time points was used for detection of secreted alkaline phosphatase. Cell lysates were used for the detection of the non-secreted alkaline phosphatase. The 20µL/ well from each sample or from medium as negative control was added to a black 96 round bottom well microplate and then incubated at 65°C for 15 min. After that, samples were cooled by incubation on ice and 20ìL of dilution buffer and 160µL of fluorescent assay buffer was added to each well. The 1µL of the substrate solution (10 mM substrate solution of 4-methylumbelliferyl phosphate disodium, 4-MUP) was added to each well and mixed. 4-Methylumbelliferyl phosphate is a substrate for alkaline phosphatase and the 4-MUP is converted to the fluorescent product 4-methylumbelliferone (4-MU), which has an emission maximum at 440 nm. Then, the microplate was read with BioTek Synergy 2 microplate reader at 360nm excitation and 440nm emission. The fluorescence intensity was measured in 96-well black microplates in six repeated experiments for each sample.

The data were normalized to the ALP activity measured using HAP control scaffold, expressed as ìmoles of 4-MU produced per min and per mg of protein, which was taken as 100% at the first time point (5d) investigated. The ALP activity obtained for each ceramic substrate at a specific time point was evaluated accordingly to the % control.

Statistical analysis

The results are reported as the arithmetic means ± standard deviations (SD) of six independent experimental values. The two-way repeated measures (RM) ANOVA and multiple comparisons by Tukey's test were applied to the results of the Alamar blue viability assay. The two-way RM ANOVA and Bonferroni post-test were applied to the results of the SIRCOL assay and ALP activity assay. The significance levels were set to $p < 0.05$, $p < 0.01$, and $p < 0.001$. All statistical analyses were performed in the GraphPad Prism 5.0 software (Graphpad, La Jolla,Ca, USA).

Results and discussions

HAP and HAP-Sr substrates (scaffolds)

The synthesized pure stoichiometric HAP: $Ca_{10}(PO_4)_6(OH)_2$ and Sr substituted hydroxyapatites. HAP-Sr: SrHAP: $Sr_{10}(PO_4)_6(OH)_2$; HAP-5%Sr: $Ca_{9.41}Sr_{0.59}(PO_4)_6(OH)_2$; HAP-10% Sr: $Ca_{8.79}Sr_{1.21}(PO_4)_6(OH)_2$; and HAP-15% Sr: $Ca_{8.13}Sr_{1.87}(PO_4)_6(OH)_2$, correspond to the general formula $Ca_{10-x}Sr_x(PO_4)_6(OH)_2$. The HAP-Sr ceramics possess a high crystallinity degree, about 68% to 86%, increasing with the Sr content in HAP lattice, as previously determined by XRD measurements [11]. The pure stoichiometric HAP has 78.5% crystallinity degree. XRD analysis clearly showed the patterns of HAP in all synthesized powders, calcined up to 850 °C, consisting of monophasic HAP and HAP-Sr, formed of thermally stable nanoparticles. Particle size is in nano scale, as follows: 61 nm for HAP, 64 nm for HAP-5wt%Sr; 76 nm for HAP-10wt%Sr; 69 nm for HAP-15wt%Sr; and 97 nm for HAP-59.2wt% Sr, as determined by TEM and AFM imaging.

In order to investigate the morphology and chemical composition of HAP and HAP-Sr substrates, the thin films deposited on a carbon coated copper grid were explored by SEM and EDX spectra. Representative SEM micrographs and EDX spectra are given in figure 1, for HAP-5%Sr substrate (a, b, e) and for HAP-10%Sr substrate (c, d, f).

The HAP-5%Sr (e) and HAP-10%Sr (f) substrates were composed of crystalline nano sized needle like particles, characterized by densified particles and nano porosity. The morphology of coating thin film of HAP-5%Sr substrate showed more compact granulated surface (a, e) than of HAP-10%Sr substrate (c, f).

The qualitative investigation of elemental composition of the coating substrates in terms of Ca, P, C, O and Sr content were performed by SEM-EDX analysis. The deposited films of HAP-Sr are characterized by the Ca+Sr: P molar ratio of about 1.67 which is close to 1.667 specific for pure stoichiometric HAP. These results are in total agreement with XRD findings that evidence the monophasic Sr substituted hydroxyapatites, preserving HAP structure.

The topography of the surface of coating films deposited on glass was examined by AFM imaging in tapping mode. A representative example is shown in figure 2, for HAP-5%Sr scaffold, as thin film deposited on glass flat plate, characterized by a mean surface roughness (e.g., root mean square: RMS) of about 9 nm ± 2 nm. The AFM images revealed that the HAP and HAP-Sr substrates are composed of nano particles in good agreement with the previous XRD and TEM data [11]. They are assembled in aggregates and grains (fig. 2, a-c) as also visualized by SEM images in figure 1. From cross-sections in AFM images on HAP and HAP-Sr deposited films on glass, the average nanoparticle size was determined. For instance, the average nanoparticle size of 64 ± 6 nm was measured for HAP-5%Sr scaffold, and it is illustrated in figure 2d.

In addition, the thickness of these scaffolds was determined by AFM to be around 1.2 μm; for example: 1.1 μm ± 0.2 μm for HAP-5%Sr and 1.2 μm ± 0.1 μm for HAP-10%Sr. The small difference in thickness between HAP-

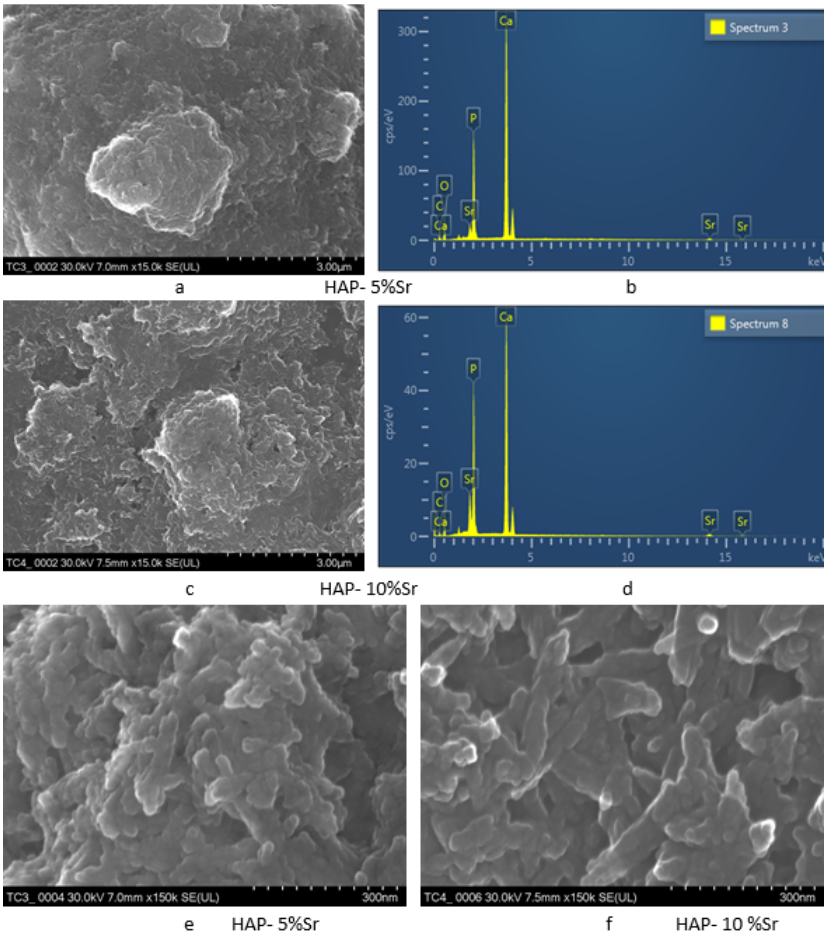

Fig. 1. SEM micrographs and EDX spectra for substrates of calcined lyophilized HAP-5%Sr (a, b, e) and HAP-10%Sr (c, d, f).

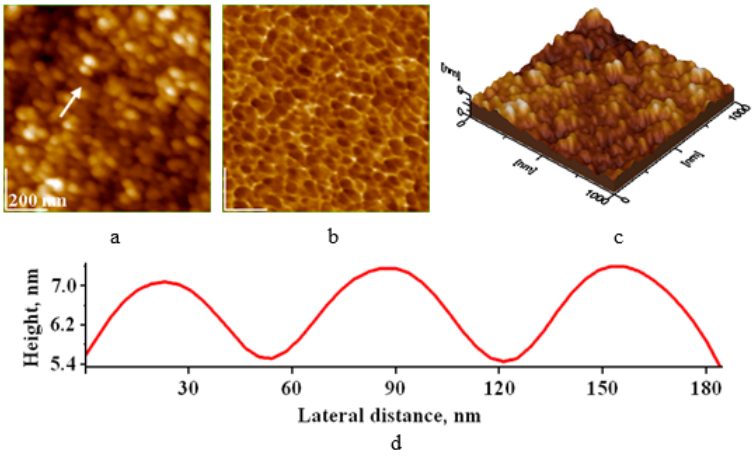

Fig. 2. AFM images of HAP-5%Sr scaffold: (a) 2D-topography, (b) phase, (c) 3D-topography, (d) cross section profile along the arrow in panel (a); scanned area 1μm x 1 μm

5%Sr and HAP-10%Sr substrates could be attributed to the different compactness of ceramic nanoparticles, in good agreement with SEM images (fig. 1, e and f). The obtained scaffold thickness is similar to the thickness of coatings on metallic implants of about 1.5 μm, which is considered proper [39] for biomedical applications,

In vitro biocompatibility tests

Fluorescein diacetate and Alamar Blue cell viability assays

The fluorescein diacetate (FDA) and Alamar Blue viability tests were performed in order to study cell adhesion (in the first few hours after seeding, 1.5h and 6h, respectively) and cell proliferation at different points of time (figs. 3-6), using as a control the cells grown on pure stoichiometric HAP scaffold. After 1.5h of cells' seeding on the surface of substrates (scaffolds), it was observed that HAP-5%Sr and HAP-10% Sr were the most favourable for the initiation of cell adhesion as FDA staining showed (fig. 3). The adhered osteoblasts on ceramic scaffolds were observed with fluorescence inverted microscope.

At 24 h (1d) the cells number increased with fairly the same advantage for HAP- 5%Sr and HAP-10%Sr (fig.4). Then, at 3 days (3d) of cultivation the most suitable for cell proliferation seemed to be pure HAP-5%Sr and especially HAP-10% Sr.

Comparing the control pure HAP with SrHAP (i.e., Ca totally replaced with Sr within HAP lattice) it is to be observed that the HAP was slightly more favourable, as judged by FDA staining, figures 3-5, and by Alamar blue viability test, figure 6, even after 12 days (12d) of cultivation. Further, Alamar blue test showed also that a relatively high amount of Sr (5wt% and 10wt%) within HAP lattice is more favourable in terms of cell viability and proliferation especially in first 5 days (5d) of cultivation. After 12d, the viability of cells on all substrates HAP-Sr with different amount (5%, 10%, 15%) of Sr was quite similar, and no statistical differences were determined (fig. 6). Additionally, all HAP-Sr and Sr-HAP nanostructured substrates didn't show any adverse effects on the

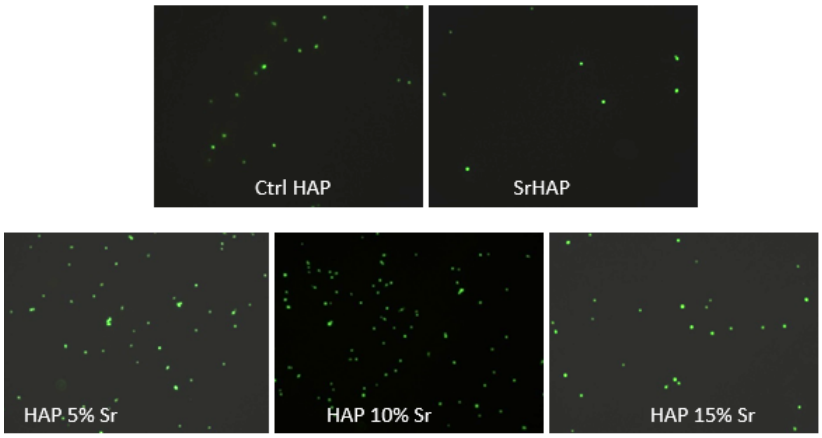

Fig. 3. FDA staining of osteoblasts after 1.5 h (1.5h) of cell seeding onto the surface of substrates, made of HAP: $Ca_{10}(PO_4)_6(OH)_2$ as a control; SrHAP: $Sr_{10}(PO_4)_6(OH)_2$; HAP-5%Sr: $Ca_{9.41}Sr_{0.59}(PO_4)_6(OH)_2$; HAP-10%Sr: $Ca_{8.79}Sr_{1.21}(PO_4)_6(OH)_2$; HAP-15%Sr: $Ca_{8.13}Sr_{1.87}(PO_4)_6(OH)_2$.

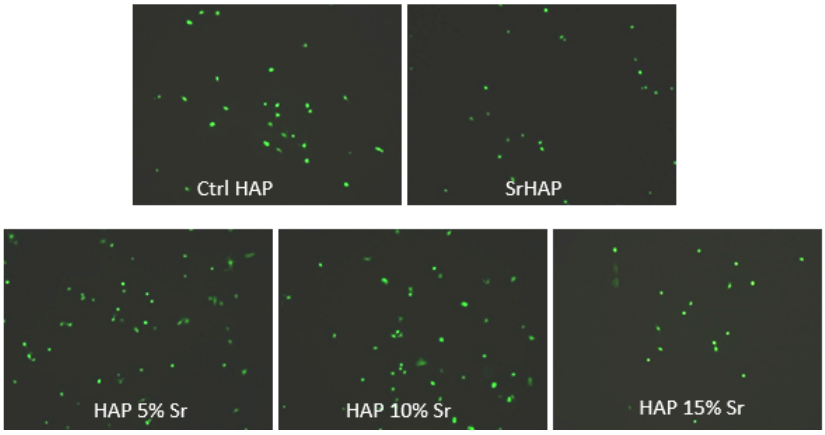

Fig. 4. FDA viability test of osteoblasts after 24 hours (1d) of cultivation on the surface of substrates, made of HAP and HAP-Sr; symbols as infigure 3

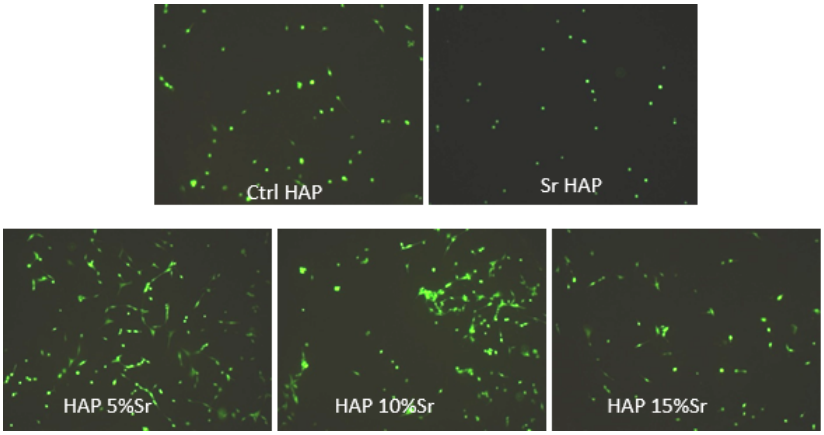

Fig. 5. FDA staining of osteoblasts after 3d of cultivation onto substrates; symbols as in figure 3

osteoblastic cell functions. Therefore, these nanostructured bio-ceramics showed a good *in vitro* biocompatibility.

In vitro response of human osteoblasts, cultured on strontium substituted hydroxyapatites, expressed in cellular viability (% control) determined by Alamar blue test, was dependent on Sr amount within HAP structure (fig.6). The control was pure HAP substrate taken as 100% at every investigated time point (fig. 6b).

Alamar blue viability test showed that HAP-Sr substrates promoted an increased cell adhesion at 6h and an enhanced cell proliferation at 1d and 3d, as presented in Figure 6a, in total agreement with FDA investigation (fig. 3-5). Increased viability values in correlation with time factor (statistically for various significance levels, $p < 0.001$, $p < 0.01$, $p < 0.05$) were observed on each HAP-Sr substrate up to day 5 (fig. 6a), where the highest value was found in the presence of HAP-10% Sr substrate, as also illustrated in figure 6b, suggesting the high proliferation of osteoblastic cells. At 12d, the obtained viability values were lower (fig. 6), probably due to the occurrence of the

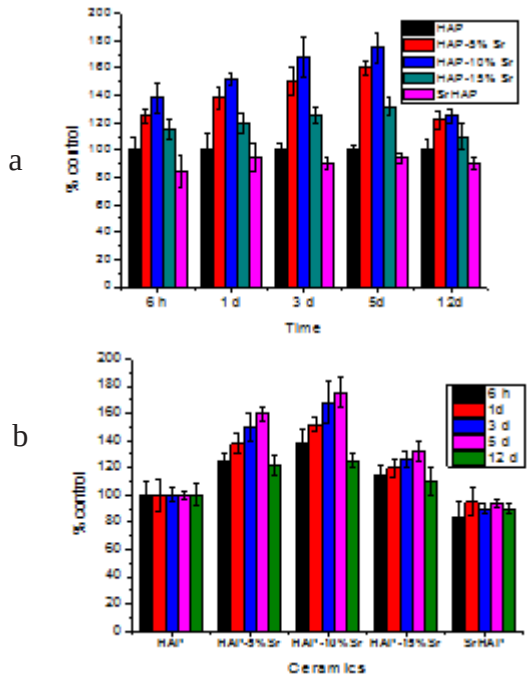

Fig. 6. Graphical aspect of viability test by Alamar blue assessed at different points of time (a) and for various substrates (b).

osteoblastic cell differentiation process, associated with a decreased cell proliferation.

Further, the results of statistical analysis revealed that there were statistical difference of cell viability among different time points and statistical differences were found among different ceramics.

While, the effects of HAP and Sr-HAP were not significantly different on the biological behavior of osteoblasts, expressed in cell proliferation, the effects of HAP-5%Sr, HAP-10%Sr and HAP-15%Sr were significantly greater than those of the HAP and Sr-HAP. The results of two-way RM ANOVA analysis showed that there were no statistical difference between the cell viability ($p > 0.05$) for HAP and Sr-HAP. Further, the results of statistical analysis showed that there were statistical differences of cell viability between HAP and HAP-5%Sr ($p < 0.001$) as well as between HAP and HAP-10% Sr ($p < 0.001$), but not significant differences between HAP and HAP-15%Sr ($p>0.05$). The cellular viability in the presence of HAP-5%Sr or of HAP-10%Sr was significantly higher ($p<0.01$) than that in the presence of Sr-HAP. The cell viability in the presence of HAP-15%Sr substrate was also significantly different than that in the presence of Sr-HAP, but at a lower level of significance ($p < 0.05$) than that corresponding for HAP-5%Sr or HAP-10%Sr substrates. The effects of HAP-5%Sr are not significantly different than those of HAP-10%Sr ($p>0.05$) on cell proliferation. The effects of HAP-5%Sr are not significantly different than those of HAP-15%Sr ($p>0.05$) on cell proliferation. However, the effects of HAP-10%Sr were greater than those of HAP-15%Sr at the significance level of $p<0.01$.

Assessing the mineralization process

SIRCOL test

Soluble type 1 collagen levels were determined by SIRCOL test at two points of time, after 5d and 21d of cultivation of osteoblasts on pure HAP, $Ca_{10}(PO_4)_6(OH)_2$ as a control, SrHAP: $Sr_{10}(PO_4)_6(OH)_2$; HAP-5%Sr: $Ca_{9.41}Sr_{0.59}(PO_4)_6(OH)_2$; HAP-10% Sr: $Ca_{8.79}Sr_{1.21}(PO_4)_6(OH)_2$; HAP-15% Sr: $Ca_{8.13}Sr_{1.87}(PO_4)_6(OH)_2$ substrates. The results revealed that the HAP-5%Sr and HAP-10%Sr substrates had better effect on the growth of osteoblasts and they presented the highest soluble collagen production at 21d (fig. 7). This favorable situation for HAP-5%Sr and HAP-10%Sr substrates can be correlated with their lower crystal stability than that of pure stoichiometric HAP, which made them more appropriate for ions release in the medium. Our previous results on ions release showed that the doping with ions of HAP lattice made it easier to be decomposed in water, and in simulated body fluid, SBF [40, 41] than that lattice in stoichiometric pure HAP. Certainly, the doping of HAP lattice with Sr can also facilitate ions release in the environment characteristic for *in vitro* and *in vivo* situations and thus, stimulating de osteoblast functions to form new bone. Therefore, these nanostructured ceramics might have applications for bone repair and regeneration.

The two-way RM ANOVA was used to determine the statistical significance and the differences were considered

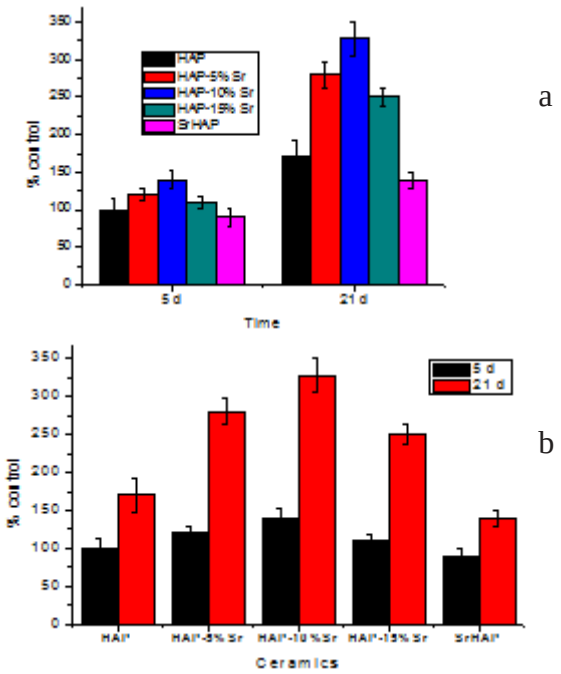

Fig. 7. Soluble collagen detection in supernatants using Sircol test at different points of time (a) and for various substrates (b)

statistically significant at $p < 0.001$, in correlation with time factor. The dosage of soluble collagen by the Sircol test in cell culture supernatants revealed the highest level of collagen for cells grown on the HAP-10% Sr substrate at 5d and at 21d. The level of collagen present in the medium has increased over this time for more than 2 times for HAP-5% Sr, HAP-10% Sr and HAP- 15% Sr substrates.

More specific, at 21d versus 5d, collagen amount increased nearly 1.7 times for pure stoichiometric HAP, 2.3 times for HAP- 5% Sr, 2.4 times for HAP-10% Sr, 2.2 times for HAP- 15% Sr, and about 1.5 times for Sr-HAP. The differences between mean values were statistically significant at $p < 0.001$, in correlation with time factor.

Alkaline phosphatase, ALP, activity

The ALP activity was quantitatively measured after 5d and 21d of osteoblasts cultivation onto substrates and it is given in figure 8. The ALP activity data were normalized to the ALP activity measured for pure stoichiometric HAP scaffold, chosen as control, which was expressed as 100% at day 5, Further all ALP activity data are expressed as % control.

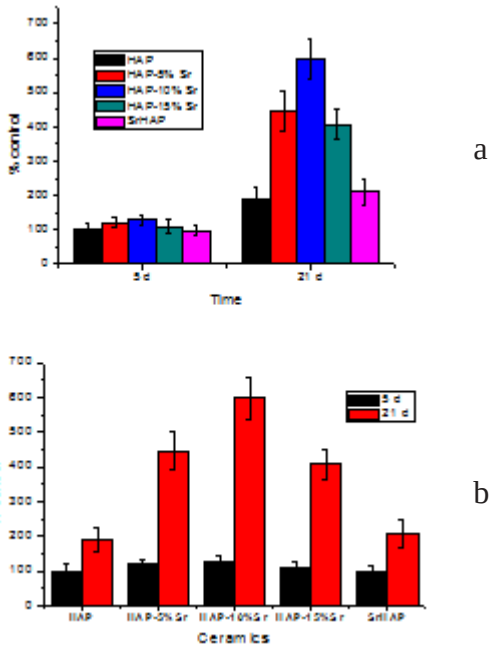

Fig. 8. Alkaline phosphatase activity at different points of time (a) and for HAP and HAP-Sr substrates (b).

A stronger ALP activity was observed for HAP-5%Sr and especially for HAP-10%Sr, at 21d of cell cultivation on scaffolds (fig.8), with a similar trend as that obtained for soluble collagen detection (fig. 7).

The ALP activity of osteoblasts on ceramics was considerably increased with time from 5d to 21d (fig. 8a). Among the different ceramics, the highest value was reached on HAP-10%Sr, at 5d and particularly at 21d (fig. 8b). The results of two-way RM ANOVA analysis showed that there was no statistical difference between the ALP activity values at 5d ($p > 0.05$) among HAP, HAP-15%Sr and Sr-HAP. Further, the results of statistical analysis at 5d showed that there was statistical differences of ALP activity between HAP and HAP-5%Sr ($p < 0.05$) as well as between HAP and HAP-10% Sr ($p < 0.001$).

Furthermore, there were significant remarkable differences of ALP activity at different time points, at 5d versus 21d, ($p < 0.001$) for each ceramic substrate. Also significant differences at 21d were found among various ceramics, as following, for $p<0.001$ among HAP, HAP-5%Sr, HAP-10%Sr and HAP-15%Sr, and $p <0.05$ for HAP compared to Sr-HAP.

The ALP activity assessed with the ALP fluorescence kit showed at 21d the highest value for HAP-10%Sr. At 21d in comparison with 5d, ALP activity increased nearly 2-fold for pure stoichiometric HAP, 3.8 times for HAP- 5% Sr, 4.6 times for HAP -10% Sr, 3.6 times for HAP- 15% Sr, and about 2 times for Sr-HAP. The differences between mean values were statistically significant for $p < 0.001$, in correlation with time factor.

The effects of HAP and Sr substituted HAP, containing various Sr amounts, as substrates in cell culture, on osteoblasts behaviour was assessed using viability tests with fluorescein diacetate and Alamar Blue, in order to evaluate the cell adhesion capacity and sustaining ability of cell proliferation and growth. *In vitro* mineralisation process was investigated by the soluble collagen type 1 production, determined by using SIRCOL test, and ALP activity evaluated by ALP fluorescent kit.

The cell viability tests, FDA staining, figures 3-5, and Alamar Blue, figures 6, showed that HAP-5% Sr, HAP-10% Sr and HAP-15%Sr were favourable in terms of cell adhesion at 1.5h and 6h, respectively, after cell seeding onto the surface of these ceramic substrates. Among these substrates HAP-5%Sr and particularly HAP-10% Sr appeared the most favourable for the adhesion, viability and growth of osteoblasts after the 3d (fig. 5) in agreement with Alamar Blue test (fig. 6). At 5d of cell cultivation the most suitable for cell proliferation seemed to be HAP-5%Sr and HAP-10%Sr (fig. 6). The osteoblast proliferation is higher on HAP-10%Sr substrate than that on pure HAP and Sr-HAP substrates. Comparing the control HAP with Sr-HAP, it is clear that the HAP was more favourable even after 12 days of cultivation (fig. 6a).

The results showed that all investigated ceramic substrates were non toxic, and they sustained the cell proliferation and viability even at 21d, when the collagen production (fig. 7) and ALP activity (fig. 8) were very high compared to their values at 5d. Alkaline phosphatase is a key enzyme strongly implicated in bone mineralization process, This enzyme was strongly activated at 21 days especially on HAP-5%Sr and HAP-10%Sr substrates (fig. 8) indicating that these ceramic substrates can promote a strong osteogenic differentiation of osteoblasts *in vitro*. This remarkable finding is in total agreement with osteogenesis

effects of different coatings made of related HAP-Sr nanomaterials used recently *in vitro* and *in vivo* applications [42].

Conclusions

The response of osteoblasts cultured on HAP and HAP-Sr demonstrated a high osteogenic potential of these ceramics and their strong involvement in bone formation and mineralization. These ceramic substrates stimulated the bone cells to grow on their surface and to actively participate in new bone formation. These substrates are osteoconductive and favour bone growth on their surface, leading osteoblasts to enter in terminal stages of differentiation triggering the mineralization process of new formed bone.

All tested ceramic substrate were biocompatible with significant differences in terms of cell adhesion, proliferation and differentiation. These results showed that HAP-Sr, particularly those with Sr amount of 5, 10% and 15%, had better biocompatibility and had an excellent osteoconductivity. However, HAP-10%Sr scaffold appeared more efficient in cell adhesion, collagen production and ALP activity, and might induce a more accelerated differentiation into osteocytes and faster construction of bone matrix.

These data are the first to reveal the specific effects of these bio-ceramics of well-defined high crystallinity on osteogenesis. These results provide a rather strong evidence for the choice of the best structure of Sr substituted HAP for the bone repair and regeneration.

Acknowledgements: The research was carried out with financial support from UEFISCDI trough the research grant no. 83. We thank to O. Horovitz for useful discussions. We thank to L. Barbu-Tudoran for SEM assistance.

References

1. POLO-CORRALES, L., LATORRE-ESTEVES, M., RAMIREZ-VICK, J.E., J. Nanosci. Nanotechnol., **14**, no. 1, 2014, p. 15.
2. O'NEILL, E., AWALE, G., DANESHMANDI, L., UMERAH, O., LO, K.W.H., Drug Discovery Today, **23**, 2018. p. 879.
3. RATNAYAKE, JT.B., MUCALO, M., DIAS, G.J.. J. Biomed. Mater. Res. Part B, **105B**, 2017, p.1285.
4. RAN, J., JIANG, P., SUN, G., MA, Z., HU, J., SHEN, X., TONG, H., Mater. Chem. Front**.,** **1**, 2017, p. 900.
5. BABA, I.Y.M., WIMPENNY, I.., BRETCANU, O., DALGARNO, K., EL HAJ, A.J., J. Biomed. Mater. Res. Part A, **105A**, 2017, p. 1775.
6. TOMOAIA, G., MOCANU, A., VIDA-SIMITI, I., JUMATE, N., BOBOS, L.D., SORITAU, O., TOMOAIA-COTISEL, M., Mater. Sci. Eng, C. **37**, 2014. p. 37.
7. MOCANU, A., FURTOS, G., RAPUNTEAN, S., HOROVITZ, O., FLORE, C., GARBO, C. DANISTEANU, A., RAPUNTEAN, G., PREJMEREAN, C., TOMOAIA-COTISEL, M., Appl. Surf. Sci., **298**, 2014, p. 225.
8. TOMOAIA, G., SORITAU, O., TOMOAIA-COTISEL, M., POP, L.B., POP, A., MOCANU, A., HOROVITZ, O., BOBOS, L.D., Powder Technol., **238**, 2013, p. 99.
9. TOMOAIA, G., TOMOAIA-COTISEL, M., POP, L.B., POP, A., HOROVITZ, O., MOCANU, A., JUMATE, N., BOBOS, L.D., Rev. Roum. Chim. **56**, no. 10-11, 2011, p. 1039.
10. GARBO, C., SINDILARU, M., CARLEA, A., TOMOAIA, G., ALMASAN, V., PETEAN, I., MOCANU, A., HOROVITZ, O., TOMOAIA-COTISEL, M., Particulate Sci. Technol., **35**, 2017, p. 29.
11. FRANGOPOL, P.T., MOCANU, A., ALMASAN, V., GARBO, C., BALINT, R., BORODI, G., BRATU, I., HOROVITZ, O., TOMOAIA-COTISEL, M., Rev. Roum. Chim. **61**, no. 4-5, 2016, p. 337.
12. FRASNELLI M, CRISTOFARO F, SGLAVO VM, DIRÈ S, CALLONE E, CECCATO R, BRUNI, G., CORNAGLIA, A.I., VISAI, L., Mater. Sci. Eng. C, **71**, 2017, p. 653.
13. CAPUCCINI C, TORRICELLI P, SIMA F, BOANINI E, RISTOSCU C, BRACCI B, SOCOL, G., FINI, M., MIHAILESCU, I.N., BIGI, A., Acta Biomater., **4**, 2008, p. 1885.
14. GUSTAVSSON, J., GINEBRA, M.P., PLANELL, J., ENGEL, E., J. Mater. Sci.: Mater. Med. **23**, 2012, p. 2509.
15. GOGA, F., FORIZS, E., AVRAM, A., ROTARU, A., LUCIAN, A., PETEAN, I., MOCANU, A., TOMOAIA-COTISEL, M., Synthesis and thermal treatment of hydroxyapatite doped with magnesium, zinc and silicon, Rev. Chim. (Bucharest), **68**, no. 6, 2017, p. 1193.
16. GOGA, F., FORIZS, E., BORODI, G., TOMOAIA, G., AVRAM, A., BALINT, R., MOCANU, A., HOROVITZ, O., TOMOAIA-COTISEL, M., Rev. Chim. (Bucharest), **68**, no. 12, 2017, p. 2907.
17. SAIDAK, Z., MARIE, P.J., Pharmacology and Therapeutics, **136,** no. 2, 2012, p. 216.
18. MARIE, P.J., Bone. **46**, no. 3, 2010, p. 571.
19. ZHAO, S.. ZHANG J., ZHU M., ZHANG Y., LIU Z., TAO, C., ZHU, Y., ZHANG, C., Acta Biomater. **12**, 2015 p. 270.
20. MURPHY, S., WREN, A.W., TOWLER, M.R., BOYD, D.. J. Mater. Sci. Mater. Med., **21**, no. 10, 2010, p. 2827.
21. SANTOCILDES-ROMERO, M.E., CRAWFORD, A., HATTON, P.V., GOODCHILD, R.L., REANEY, I.M., MILLER, C.A., J. Tissue Eng. Regen. Med., **9**, no. 5, 2015, p. 619.
22. MARIE, P.J., AMMANN, P., BOIVIN G., REY, C., Calcif. Tissue Int., **69**, 2001, p. 121.
23. PILMANE, M., SALMA-ANCANE K., LOCA D., LOCS, J., BERZINA-CIMDINA, L, Mater. Sci. Eng. C, **78**, 2017, p. 1222.
24. BIGI, A., BOANINI, E., CAPUCCINI, C., GAZZANO, M.. Inorg. Chim. Acta, **360**, 2007, p. 1009.
25. ZHANG, W., SHEN, Y., PAN, H., LIN, K., LIU, X., DARVELL BW., LU, W.W., CHANG, J., DENG, L., WANG, D., HUANG, W., Acta Biomater., **7**, no. 2, 2011 p. 800.
26. LANDI, E., TAMPIERI, A., CELOTTI, G., SPRIO, S., SANDRI, M., LOGROSCINO, G., Acta Biomater. **3**, 2007, p. 961.
27. NI, G.X., CHIU, K.Y., LU, W.W., WANG, Y., ZHANG, Y.G., HAO, L.B., LI, Z.Y., LAM, W.M., LU, S.B., LUK, K.D., Biomaterials. **27**, no. 24, 2006, p. 4348.
28. NI, G.X., YAO, Z.P., HUANG, G.T., LIU, W.G., LU, W.W. J. Mater. Sci.: Mater. Med., **22**, 2011, p. 961.
29. MOURINO, V., CATTALINI, J.P., BOCCACCINI, A.R. J. Roy. Soc. Interface, **9**, no. 68, 2012, p. 401.
30. GALLAGHER, J.A., GUNDLE, R., BERESFORD, J.N., Methods Mol. Med., **2**, 1996, p. 233.
31. TOMOAIA, G., POP, L.B., PETEAN, I., TOMOAIA-COTISEL, M., Mater. Plast. **49**, no. 1, 2012, p. 48.
32. HOROVITZ, O., TOMOAIA, G., MOCANU, A., YUPSANIS, T., TOMOAIA-COTISEL M., Gold Bull. **40,** no. 4, 2007, p. 295.
33. TOMOAIA, G., HOROVITZ, O., MOCANU, A., NITA, A., AVRAM, A., RACZ, C.P., SORITAU, O., CENARIU, M., TOMOAIA-COTISEL, M., Colloids Surf, B. **135**, 2015, p. 135.
34. TOMOAIA-COTISEL, M., TOMOAIA-COTISEL, A., YUPSANIS, T., TOMOAIA, G., BALEA, I., MOCANU, A., RACZ, C., Rev. Roum. Chim., **51,** no. 12, 2006, p. 1181.
35. COJOCARU, I., TOMOAIA-COTISEL, A., MOCANU, A., YUPSANIS, T., TOMOAIA-COTISEL, M., Rev. Chim. (Bucharest), **68**, no. 7, 2017, p. 1470.
36. FRANGOPOL. P.T., CADENHEAD, D.A., TOMOAIA, G., MOCANU, A., TOMOAIA-COTISEL, M., Rev. Roum.Chim., **60**, no. 2-3, 2015, p. 265.
37**.** MOCANU, A., PASCA, R.D., TOMOAIA, G., GARBO, C., FRANGOPOL, P.T., HOROVITZ, O., TOMOAIA-COTISEL, M., Internat. J. Nanomed., **8**, 2013, p. 3867.
38. TOMOIA, G., FRANGOPOL, P.T., HOROVITZ, O., BOBOS, L.D., MOCANU, A., TOMOAIA-COTISEL, M., J. Nanosci. Nanotechnol., **11**, no. 9, 2011, p. 7762.
39. RAU, J.V., FOSCA, M., CACCIOTTI, I., LAURETI, S., BIANCO, A., TEGHIL, R. Thin Solid Films, **543**, 2013, p. 167**.**
40. CADAR, O., FRANGOPOL, P.T., TOMOAIA, G., OLTEAN, D., PALTINEAN, G.A., MOCANU, A., HOROVITZ, O., TOMOAIA-COTISEL, M., Studia Univ. Babes-Bolyai, Chemia, **62**, no. 4 (Tom 1), 2017, p. 67.
41. CADAR, O., BALINT, R., TOMOAIA, G., FLOREA, D., PETEAN, I., MOCANU, A., HOROVITZ, O., TOMOAIA-COTISEL, M., Studia Univ. Babes-Bolyai, Chemia, **62**, no. 4 (Tom 2), 2017, p. 269.
42. MAO, L., XIA, L., CHANG, J., LIU, J., JIANG, L., WU, C., FANG, B., Acta Biomaterialia, **61**, 2017, p. 217.

Manuscript received: 17.08.2018